Correlation between superconductivity and antiferromagnetism in $Rb_{0.8}Fe_{2-y}Se_{2-x}Te_x$ single crystals

Dachun Gu, Liling Sun,* Qi Wu, Chao Zhang, Jing Guo, Peiwen Gao, Yue Wu, Xiaoli Dong, Xi Dai, and Zhongxian Zhao*
Institute of Physics and Beijing National Laboratory for Condensed Matter Physics, Chinese Academy of Sciences, Beijing 100190, China
(Received 13 July 2011; revised manuscript received 10 May 2012; published 23 May 2012)

We report experimental evidence for the connection between superconductivity and antiferromagnetism in $Rb_{0.8}Fe_{2-y}Se_{2-x}Te_x$ single crystals under negative chemical pressure introduced by the lattice expansion of substituting Se with isovalent Te atoms. Electrical resistance and magnetic measurements in the temperature range from 4 to 600 K demonstrate that both superconducting transition temperature (T_c) and the Neel temperature (T_N) are suppressed continuously with the lattice expansion. When the Te concentration x in $Rb_{0.8}Fe_{2-y}Se_{2-x}Te_x$ approaches 0.4, the superconductivity is completely suppressed, and the sample behaves like a semiconductor; meanwhile, the features for antiferromagnetic transition on resistance and magnetization curves disappear. Our observation suggests that the effect of negative-pressure-induced lattice expansion can be used to tune the correlativity of superconductivity and antiferromagnetism in the studied system.

DOI: 10.1103/PhysRevB.85.174523 PACS number(s): 74.70.Xa, 74.62.Fj

The discovery of superconductivity in $LaFeAsO_{1-x}F_x$ with T_c as high as 26 K[1] has attracted considerable attention in the communities of condensed matter physics and material science. During the past four years, several other types of iron-based superconductors with 122 structure (MFe_2As_2, M = Ca, Sr, Ba, and Eu),[2–5] 111 structure (AFeAs, A = Li and Na),[6,7] 11 structure (FeSe),[8] and 42622 structure ($Sr_4V_2O_6Fe_2As_2$)[9] were found. Among them, the highest T_c has reached as high as 55 K in $SmFeAsO_{1-x}F_x$.[10] Recently, another new family of superconductors $M_xFe_{2-y}Se_2$ (M = K, Rb, Cs, or Tl substituted K, Rb) with T_c above 30 K and other unusual features was discovered,[11–15] which simulated great interest in the communities. The $M_xFe_{2-y}Se_2$ superconductors show a number of peculiar features, including electron-dominated carriers in the Fermi surface,[16–19] high-transition temperature of antiferromagnetic phase, superstructure of Fe vacancies, and large ordering magnetic moment for each iron atom.[20,21] Application of internal or external positive pressure on these superconductors showed that the superconducting transition temperature is suppressed with increasing pressure;[22–24] especially recent investigations demonstrate that external physical pressure can tune the T_c down continuously until approaching a quantum critical point (QCP).[22] Moreover, a reemerging superconductivity appears after the pressure is above the QCP,[25] which enhances the mystery of these kinds of superconductors. In this paper, we investigate the effect of negative pressure introduced by substituting selenium (Se) with isovalent tellurium (Te) in $Rb_{0.8}Fe_{2-y}Se_2$. We found that superconductivity and the Neel temperature are suppressed with Te doping. When the doping concentration of Te approaches 0.4, the superconductivity vanishes; meanwhile, its antiferromagnetic order almost disappears. This indicates the existence of an interconnection between superconductivity and antiferromagnetism in this material. By comparison with positive pressure effect, we propose that a pressure-free sample (applied neither positive nor negative pressure) possesses an optimal lattice and electron structure configurations which are in favor of optimal superconductivity.

Single crystals of $Rb_{0.8}Fe_{2-y}Se_{2-x}Te_x$ were grown by a self-flux method with several steps. First, precursors of FeSe and FeTe were synthesized by solid reaction method. High-purity Fe, Se, and Te powders were mixed together with nominal composition of Fe : Se and Fe : Te in a mortar. The mixture was put into a furnace and heated to 700 °C with a rate of 100 °C/hour, kept at this temperature for 24 h, and then cooled down to room temperature naturally. Secondly, the precursors were mingled with Rb in a glovebox and loaded into an alumina crucible, then sealed in an evacuated silica ampoule. Thirdly, the sealed silica tube was placed in a furnace, slowly heated to 1000 °C and kept at this temperature for 5 h, afterward heated up to 1100 °C and kept for another 5 h. Finally, the samples were cooled down to 800 °C with a rate of 4 °C/hour, followed by shutting off the power of the furnace.

The resulting samples were characterized by x-ray diffractometer Rigaku Ultima IV with Cu Kα radiation (λ = 1.5418 Å) in the 2θ scan mode [Fig. 1(a)]. Sharp (00l) peaks reflect that the sample orientates well in the c direction. Powder x-ray diffraction was also carried out in the same diffractometer [Fig. 1(b)]. The sample ground from the same batch of the single crystal was measured by step scanning in the range from 10° to 120° in 2θ with sampling intervals of 0.02°, and the accumulation time was one minute for each degree. Rietveld refinements of the data were performed using the FULLPROF package.

Electrical resistance and magnetic susceptibility measurements below 300 K were performed with a physical property measurement system (PPMS-9) and a superconducting quantum interference device (SQUID-XL1). As shown in Figs. 1(c) and 1(d), clear superconducting transitions at 31.4 K determined by the resistance measurement and at 30.2 K detected by the magnetic susceptibility measurement were observed, indicating a bulk nature of superconductivity in $Rb_{0.8}Fe_{2-y}Se_2$.

The actual chemical composition for all samples was characterized by inductive coupled plasma-atomic emission spectrometer, the resulting composition of which is listed in the Table I. It is seen that the actual composition of the Te concentration in the studied sample is quite close to that of its nominal composition.

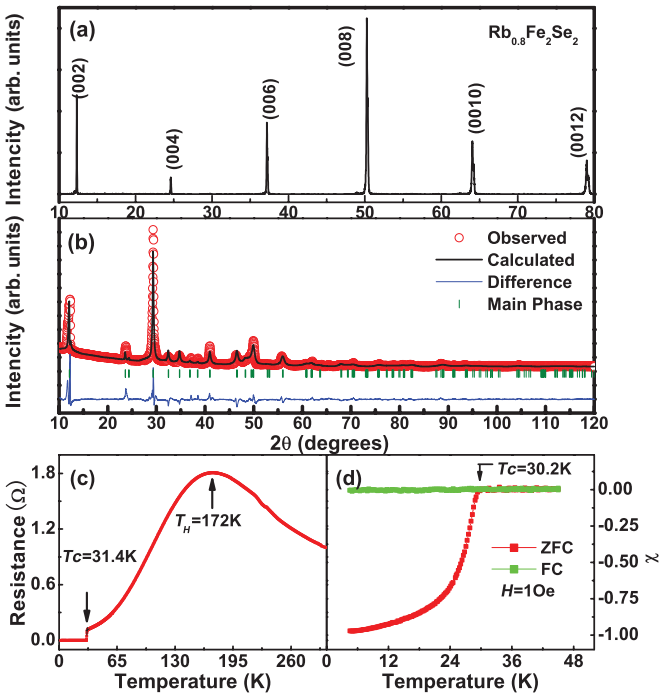

FIG. 1. (Color online) (a) X-ray diffraction (XRD) pattern of $Rb_{0.8}Fe_{2-y}Se_2$ single crystal, displaying only (00l) peaks. (b) XRD pattern and Rietveld refinement of the powder $Rb_{0.8}Fe_{2-y}Se_2$ ground from the same batch of the single crystal, yielding the agreement factors of the refinement $R_p = 7.29\%$, $R_{wp} = 12.1\%$, and $R_{\exp} = 2.47\%$, respectively. (c) Temperature dependence of corresponding electrical resistance. (d) Magnetic susceptibility as a function of temperature for zero-field-cooling and field-cooling processes.

To investigate how the tellurium substitution influences the lattice distortion, we first performed powder x-ray diffraction measurements at room temperature for $Rb_{0.8}Fe_{2-y}Se_{2-x}Te_x$ ($x = 0$–0.4) single crystals. As shown in Fig. 2(a), all samples can be well indexed to be tetragonal structure, demonstrating that no phase transition occurs in the substitution range investigated. However, the lattice expansion is clearly observed with increasing Te concentration [Fig. 2(b)], due to the substitution of tellurium whose ionic radius is larger than Se. The expansion in the c direction is about 1.3%, slightly larger than that (0.7%) in the a direction. Figure 2(c) shows how the volume of a unit cell grows with increasing Te concentration. The obtained data confirm that Te substitution induces a volume expansion which is equivalent to a negative pressure being applied to the system.

TABLE I. Comparison of actual and nominal composition of $Rb_zFe_{2-y}Se_{2-x}Te_x$.

Nominal composition	Actual composition
$Rb_{0.8}Fe_2Se_2$	$Rb_{0.74}Fe_{1.7}Se_2$
$Rb_{0.8}Fe_2Se_{1.9}Te_{0.1}$	$Rb_{0.78}Fe_{1.67}Se_{1.9}Te_{0.095}$
$Rb_{0.8}Fe_2Se_{1.85}Te_{0.15}$	$Rb_{0.77}Fe_{1.64}Se_{1.85}Te_{0.166}$
$Rb_{0.8}Fe_2Se_{1.8}Te_{0.2}$	$Rb_{0.83}Fe_{1.66}Se_{1.8}Te_{0.198}$
$Rb_{0.8}Fe_2Se_{1.75}Te_{0.25}$	$Rb_{0.79}Fe_{1.63}Se_{1.75}Te_{0.210}$
$Rb_{0.8}Fe_2Se_{1.7}Te_{0.3}$	$Rb_{0.82}Fe_{1.63}Se_{1.7}Te_{0.272}$
$Rb_{0.8}Fe_2Se_{1.6}Te_{0.4}$	$Rb_{0.8}Fe_{1.66}Se_{1.6}Te_{0.400}$

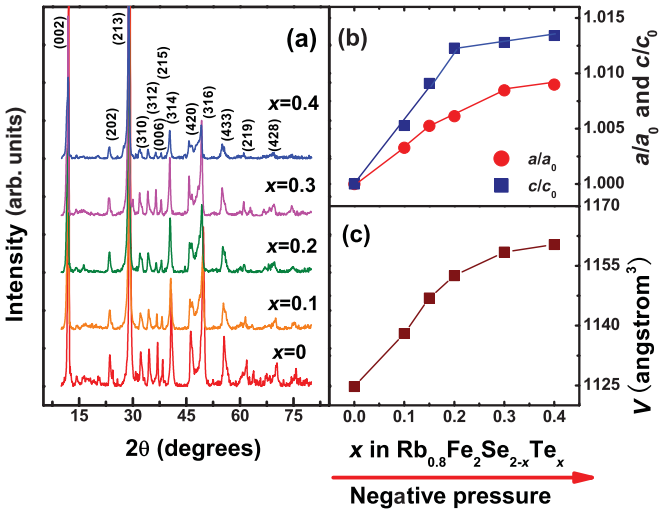

FIG. 2. (Color online) (a) X-ray diffraction patterns of powdered $Rb_{0.8}Fe_{2-y}Se_{2-x}Te_x$, which is ground from the single crystals. (b) Lattice parameters of $Rb_{0.8}Fe_{2-y}Se_{2-x}Te_x$ as a function of Te concentration. (c) Te substitution dependence of volume, showing that Te substitution expands the lattice.

Figure 3 shows the temperature dependence of electrical resistance for samples with different Te concentrations. We found that, with negative pressure increasing (x smaller than 0.25), superconducting transition temperatures (T_c) of the samples are suppressed [Fig. 3(a)]. When the Te doping approaches 0.3, it was noted that its resistance increases with declining temperature, showing a semiconductor behavior

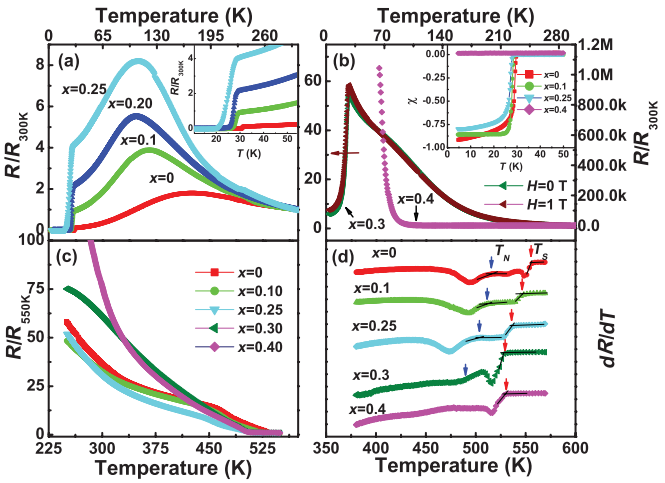

FIG. 3. (Color online) (a) Temperature dependence of resistance for $Rb_{0.8}Fe_{2-y}Se_{2-x}Te_x$ ($x = 0 \sim 0.25$) at zero magnetic field. The inset displays the enlarging view of T_c decreasing with Te substitution. (b) Resistance as a function of temperature for $Rb_{0.8}Fe_{2-y}Se_{2-x}Te_x$ ($x = 0.3$) at zero magnetic field (green color) and 1 T magnetic field (wine color), as well as resistance as a function of temperature for $Rb_{0.8}Fe_{2-y}Se_{2-x}Te_x$ ($x = 0.4$) at zero magnetic field (pink color). The inset of (b) displays dc susceptibility as a function of temperature for the samples with different Te contents. (c) High-temperature resistance measured from 250 to 550 K for $Rb_{0.8}Fe_{2-y}Se_{2-x}Te_x$ ($x = 0 \sim 0.4$). (d) The first derivation of the resistance as a function of temperature, exhibiting two important transitions.

above the temperature of 30 K, while exhibiting a drop at ~26 K. Although no zero resistance was observed, we still applied a magnetic field of 1 T to identify whether the resistance drop is related to a superconducting transition. The result shows that the resistance-temperature curve shifts to the lower temperature side under the field, as displayed in Fig. 3(b), revealing that some isolating superconducting phases may exist in the sample. In order to clarify the intrinsic behavior for the sample with $x = 0.3$, we carried out resistance measurements for four fresh samples from different batches and found the same results. When Te concentration comes to 0.4, the superconductivity is fully destroyed [Fig. 3(b)]. The suppression of T_c with increasing Te concentration is also confirmed by dc susceptibility measurements [inset of Fig. 3(b)]. The magnetic detection shows that either superconducting transition temperature or volume fraction of superconducting phase decreases with increasing negative pressure. The sample of $x = 0.4$ is no longer diamagnetic, which is very consistent with our resistance measurement.

To identify the effect of negative pressure on the long-range antiferromagnetic orders and its relation to superconductivity of the samples investigated, we measured electrical resistance from 300 to 600 K for $Rb_{0.8}Fe_{2-y}Se_{2-x}Te_x$ single crystals. The resistance and its derivative as a function of temperature were plotted in Figs. 3(c) and 3(d). We found two dips on the dR/dT curve; one is associated with the formation of Fe-vacancy order (whose transition temperature is defined as T_S), and the other is related to the antiferromagnetic phase transition (whose transition temperature is defined as T_N), as reported previously.[26] For the Te-free sample, its T_S and T_N are about 556 and 510 K, respectively, which are slightly different from the corresponding values reported in Ref. 26. This may be due to the subtle difference of sample's composition. Both T_S and T_N decrease with increasing Te concentration, indicating that the lattice expansion is in favor of suppressing the formation of Fe vacancies as well as the transition temperature of paramagnetic-to-antiferromagnetic phase. Importantly, we found that T_N vanishes from the dR/dT curve at $x = 0.4$, where the sample completely loses its superconductivity. The synchronic suppression ($x < 0.3$) and disappearance ($x = 0.4$) of T_N and T_c suggest the existence of a link between superconductivity and antiferromagnetism.

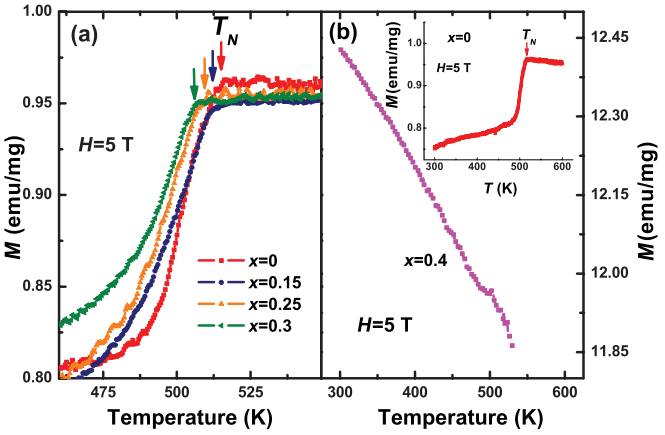

FIG. 5. (Color online) (a) Magnetization as a function of temperature measured at 5 T for $Rb_{0.8}Fe_{2-y}Se_{2-x}Te_x$ ($x = 0 \sim 0.3$), showing the suppression of antiferromagnetism with increasing Te concentration. (b) Magnetization as a function of temperature for the sample of $x = 0.4$. Inset of (b) exhibits temperature dependence of magnetization measured at 5 T in a wide temperature range (300–600 K) for the sample of $x = 0$.

The response of superconductivity to negative pressure in Te-doped $Rb_{0.8}Fe_{2-y}Se_{2-x}Te_x$ is similar to that of positive pressure in S-doped $K_xFe_{2-y}Se_2$ or compressed $K_{0.8}Fe_{1.7}Se_2$.[22–24] Figure 4 displays pressure dependences of

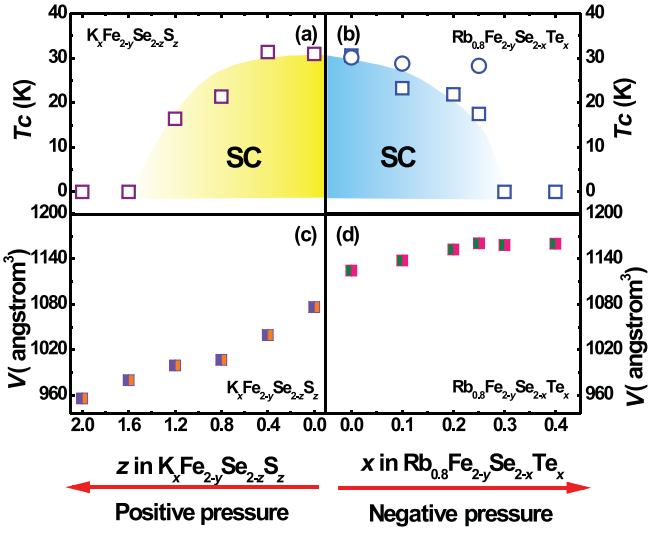

FIG. 4. (Color online) (a) and (c) The T_c and volume as a function of sulfur (S) concentration in $K_xFe_{2-y}Se_{2-z}S_z$, data in (a) and (c) are adopted from Ref. 24. (b) and (d) T_c and volume as a function of Te concentration in $Rb_{0.8}Fe_{2-y}Se_{2-x}Te_x$. The squares in (b) represent the T_c determined by resistance measurements, and the circles represent the T_c determined by dc susceptibility measurements. Here, the T_c (square) is defined by the temperature where the resistance equals to zero, and the Tc (circle) is defined by the temperature where the sample is diamagnetic.

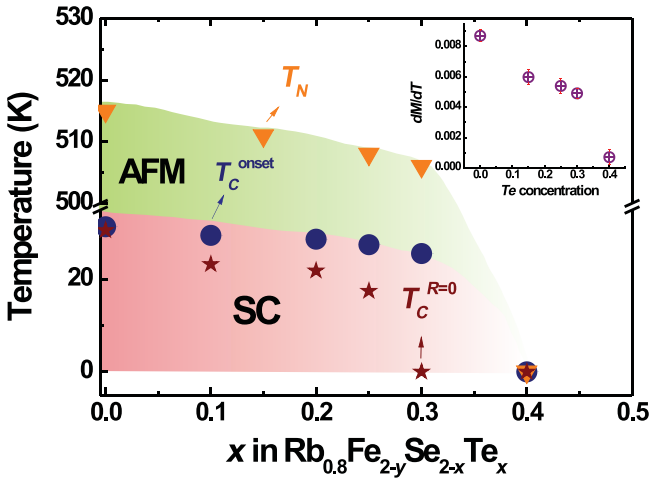

FIG. 6. (Color online) Antiferromagnetic transition temperature (T_N) and superconducting transition temperature (T_c) as a function of Te doping in $Rb_{0.8}Fe_{2-y}Se_{2-x}Te_x$ single crystals. Inset displays magnetism derivative as a function of temperature for the samples with different Te doping.

T_c and of volume for the S-doped and Te-doped samples. We found that either positive pressure or negative pressure can suppress superconductivity, but a pressure-free sample possesses an optimal superconductivity.

To further investigate negative pressure effect on T_N, we performed high-temperature magnetic measurements for all samples (Fig. 5). We found the same phenomenon, i.e. the T_N is suppressed with increasing Te concentration. Through careful inspection on temperature dependence of magnetization for each sample investigated, we found that the intensity of the antiferromagnetic transition of the studied samples is doping dependent. When the doping level reaches 0.4, the sample loses its magnetic order, which is in good agreement with our resistive detection. We summarized phase diagrams of negative pressure dependence of T_c and T_N in Fig. 6. It is obvious that both T_c and T_N decrease with increasing Te concentration. When the superconductivity completely vanishes in the sample of $x = 0.4$, its antiferromagnetic order disappears simultaneously. For the sake of further illuminating the effect of Te doping on T_N, we also plotted dM/dT as a function of Te doping (negative pressure) in the inset of Fig. 6 and found that dM/dT decreases with an enhancement of Te concentration. The results are reproducible in three independent runs with new samples. Our data indicate that once the antiferromagnetic ordering is constructed, the superconducting phase emerges at low temperature, suggesting an interconnection between superconductivity and antiferromagnetism. Recently, μsR, Mossbauer, neutron scattering, and Raman experiments also showed that the superconductivity in $M_xFe_{2-y}Se_2$ coexists with the antiferromagnetic long-range order.[20,26–29] The reported experimental finding in this study on correlation between superconductivity and antiferromagnetism in $Rb_{0.8}Fe_{2-y}Se_{2-x}Te_x$ single crystals should be important and informative for underlying superconducting mechanisms of this unusual new type of superconductors.

In summary, we show that the partial substitution of tellurium for selenium can create negative pressure, which leads to the lattice expansion. Resistance and magnetization measurements suggest that superconductivity and antiferromagnetism of $Rb_{0.8}Fe_{2-y}Se_{2-x}Te_x$ single crystals are doping dependent, i.e. both of T_c and T_N are suppressed with increasing Te concentration or increasing negative pressure. At $x = 0.4$, the superconductivity is completely destroyed, and the antiferromagnetic order almost disappears simultaneously. This suggests that the superconductivity in $Rb_{0.8}Fe_{2-y}Se_{2-x}Te_x$ is correlated to its antiferromagnetism. Summarizing the effects of positive and negative pressures on the $M_xFe_{2-y}Se_2$ superconductors, we propose that application of any kind of pressure is not in favor of their superconductivity.

We would like to thank P. C. Dai, T. Xiang, and Z. Fang for useful discussions. We acknowledge H. X. Chen and N. L. Wang for the help of magnetic measurements. This work was supported by NSCF (10874230 and 11074294), 973 projects (2010CB923000 and 2011CBA00109), and Chinese Academy of Sciences.

*Corresponding author: llsun@aphy.iphy.ac.cn and zhxzhao@iphy.ac.cn

[1] Y. Kamihara, T. Watanabe, M. Hirano, and H. Hosono, J. Am. Chem. Soc. **130**, 3296 (2008).
[2] F. Ronning, T. Klimczuk, E. D. Bauer, H. Volz, and J. D. Thompson, J. Phys.: Condens. Matter **20**, 322201 (2008).
[3] G. F. Chen, Z. Li, G. Li, W. Z. Hu, J. Dong, J. Zhou, X. D. Zhang, P. Zheng, N. L. Wang, and J. L. Luo, Chin. Phys. Lett. **25**, 3403 (2008).
[4] M. Rotter, M. Tegel, D. Johrendt, I. Schellenberg, W. Hermes, and R. Pottgen, Phys. Rev. B **78**, 020503(R) (2008).
[5] Z. Ren, Z. W. Zhu, S. Jiang, X. F. Xu, Q. Tao, C. Wang, C. M. Feng, G. H. Cao, and Z. A. Xu, Phys. Rev. B **78**, 052501 (2008).
[6] J. H. Tapp, Z. Tang, B. Lv, K. Sasmal, B. Lorenz, P. C. W. Chu, and A. M. Guloy, Phys. Rev. B **78**, 060505(R) (2008).
[7] G. F. Chen, W. Z. Hu, J. L. Luo, and N. L. Wang, Phys. Rev. Lett. **102**, 227004 (2009).
[8] F. C. Hsu, J. Y. Luo, K. W. Yeh, T. K. Chen, T. W. Huang, P. M. Wu, Y. C. Lee, Y. L. Huang, Y. Y. Chu, D. C. Yan, and M. K. Wu, Proc. Nat. Acad. Sci. **105**, 14262 (2008).
[9] X. Y. Zhu, F. Han, G. Mu, P. Cheng, B. Shen, B. Zeng, and H. H. Wen, Phys. Rev. B **79**, 220512 R (2009).
[10] Z. A. Ren, W. Lu, J. Yang, W. Yi, X. L. Shen, Z. C. Li, G. C. Che, X. L. Dong, L. L. Sun, F. Zhou, and Z. X. Zhao, Chin. Phys. Lett. **25**, 2215 (2008).
[11] J. G. Guo, S. F. Jin, G. Wang, S. C. Wang, K. X. Zhu, T. T. Zhou, M. He, and X. L. Chen, Phys. Rev. B **82**, 180520(R) (2010).
[12] A. F. Wang, J. J. Ying, Y. J. Yan, R. H. Liu, X. G. Luo, Z. Y. Li, X. F. Wang, M. Zhang, G. J. Ye, P. Cheng, Z. J. Xiang, and X. H. Chen, Phys. Rev. B **83**, 060512(R) (2011).
[13] A. Krzton-Maziopa, Z. Shermadini, E. Pomjakushina, V. Pomjakushin, M. Bendele, A. Amato, R. Khasanov, H. Luetkens, and K. Conder, Phys.: Condens. Matter **23**, 052203 (2011).
[14] M. H. Fang, H. D. Wang, C. H. Dong, Z. J. Li, C. M. Feng, J. Chen, and H. Q. Yuan, EPL **94**, 27009 (2011).
[15] H. D. Wang, C. H. Dong, Z. J. Li, Q. H. Mao, S. S. Zhu, C. M. Feng, H. Q. Yuan, and M. H. Fang, EPL **93**, 47004 (2011).
[16] Z. G. Chen, R. H. Yuan, T. Dong, G. Xu, Y. G. Shi, P. Zheng, J. L. Luo, J. G. Guo, X. L. Chen, and N. L. Wang, Phys. Rev. B **83**, 220507(R) (2011).
[17] T. Qian, X. P. Wang, W. C. Jin, P. Zhang, P. Richard, G. Xu, X. Dai, Z. Fang, J. G. Guo, X. L. Chen, and H. Ding, Phys. Rev. Lett. **106**, 187001 (2011).
[18] Y. Zhang, L. X. Yang, M. Xu, Z. R. Ye, F. Chen, C. He, H. C. Xu, J. Jiang, B. P. Xie, J. J. Ying, X. F. Wang, X. H. Chen, J. P. Hu, M. Matsunami, S. Kimura, and D. L. Feng, Nature Mater. **10**, 273 (2011).
[19] D. X. Mou, S. Y. Liu, X. W. Jia, J. F. He, Y. Y. Peng, L. Zhao, L. Yu, G. D. Liu, S. L. He, X. L. Dong, J. Zhang, H. D. Wang, C. H. Dong, M. H. Fang, X. Y. Wang, Q. J. Peng, Z. M. Wang, S. J. Zhang, F. Yang, Z. Y. Xu, C. T. Chen, and X. J. Zhou, Phys. Rev. Lett. **106**, 107001 (2011).

[20]W. Bao, Q. Huang, G. F. Chen, M. A. Green, D. M. Wang, J. B. He, X. Q. Wang, and Y. Qiu, Chin. Phys. Lett. **28**, 086104 (2011).
[21]W. Bao, G. N. Li, Q. Huang, G. F. Chen, J. B. He, M. A. Green, Y. Qiu, D. M. Wang, and J. L. Luo, e-print arXiv:1102.3674.
[22]J. Guo, X. J. Chen, J. Dai, C. Zhang, J. Guo, X. Chen, Q. Wu, D. Gu, P. Gao, L. Yang, K. Yang, X. Dai, H. K. Mao, L. Sun, and Z. Zhao, Phys. Rev. Lett. **108**, 197001 (2012).
[23]J. J. Ying, X. F. Wang, X. G. Luo, Z. Y. Li, Y. J. Yan, M. Zhang, A. F. Wang, P. Cheng, G. J. Ye, Z. J. Xiang, R. H. Liu, and X. H. Chen, New J. Phys. **13**, 033008 (2011).
[24]H. Lei, M. Abeykoon, E. S. Bozin, K. Wang, J. B. Warren, and C. Petrovic, Phys. Rev. Lett. **107**, 137002 (2011).
[25]L. L. Sun, X. J. Chen, J. Guo, P. W. Gao, Q. Z. Huang, H. D. Wang, M. H. Fang, X. L. Chen, G. F. Chen, Q. Wu, C. Zhang, D. C. Gu, X. L. Dong, L. Wang, K. Yang, A. G. Li, X. Dai, H. K. Mao, and Z. X. Zhao, Nature **483**, 67 (2012).
[26]R. H. Liu, X. G. Luo, M. Zhang, A. F. Wang, J. J. Ying, X. F. Wang, Y. J. Yan, Z. J. Xiang, P. Cheng, G. J. Ye, Z. Y. Li, and X. H. Chen, EPL **94**, 27008 (2011).
[27]Z. Shermadini, A. Krzton-Maziopa, M. Bendele, R. Khasanov, H. Luetkens, K. Conder, E. Pomjakushina, S. Weyeneth, V. Pomjakushin, O. Bossen, and A. Amato, Phys. Rev. Lett. **106**, 117602 (2011).
[28]D. H. Ryan, W. N. Rowan-Weetaluktuk, J. M. Cadogan, R. Hu, W. E. Straszheim, S. L. Bud'ko, and P. C. Canfield, Phys. Rev. B **83**, 104526 (2011).
[29]A. M. Zhang, K. Liu, J. H. Xiao, J. B. He, D. M. Wang, G. F. Chen, B. Normand, and Q. M. Zhang, Phys. Rev. B **85**, 024518 (2012).